PAPER 52 (SESSION V)

The influence of stacking fault energy on fatigue fracture

C. M. WAN, B.Sc. and Professor J. G. BYRNE

University of Utah, Salt Lake City, Utah, U.S.A.

Summary

The detailed nature of the substructural changes which occur during fatigue are being examined to determine how they are related to the morphology of the fracture surface. The controlling parameter being varied is the stacking fault energy $\gamma_{S.F.}$ of the extended dislocations in alloys of 20% and 60% Co in Ni. The material with the lower $\gamma_{S.F.}$ (60% Co) resists fatigue failure longer presumably because of the increased difficulty of dislocation cross-slip, which, in turn, retards the formation of extrusions and intrusions and hence fatigue crack nuclei.

Analysis of X-ray line broadening to multiple orders of spectra taken as a function of fatigue life at a maximum fiber stress of 45,000 psi has revealed:

1. The size of the smallest coherently diffracting domain (particle size) decreases an order of magnitude faster along $\langle 111 \rangle$ than along $\langle 100 \rangle$.
2. The particle size along $\langle 111 \rangle$ in the high $\gamma_{S.F.}$ alloy (20% Co) in turn decreases an order of magnitude faster than that along $\langle 111 \rangle$ in the low $\gamma_{S.F.}$ alloy.
3. The particle size approaches a limit of 500 Å just prior to fracture almost independently of composition or crystallographic direction.

Application of electron fractography has revealed that the distance a fatigue crack propagates per cycle is four times larger (32 cells of approximately 500 Å diameter) in the high $\gamma_{S.F.}$ material than in the lower $\gamma_{S.F.}$ material (8 cells). It is perhaps extremely significant that there is also a factor of four between the $\gamma_{S.F.}$ values of the two alloys.

Introduction

Because of the very high frequency of engineering failures which are of a fatigue nature, it behooves materials researchers to attempt to try to understand fatigue failure mechanisms in as much detail as possible. Most of the proposed intrusion-extrusion fatigue failure mechanisms invoke the cross-slip of screw dislocations and it is well known that cross-slip is dependent upon the stacking fault energy of the material. A low value of stacking fault energy permits a wide separation of the partial dislocations bounding the fault and since these must be forced together prior to cross-slip, any fatigue mechanism dependent upon such cross-slip becomes retarded. Thus in the work described here two solid-solution Ni-Co alloys, nominally 20% and 60% Co, were selected for study since the main difference between them is that the 20% Co alloy has a stacking fault energy about four times higher than that of the 60% Co alloy [1]. This

investigation then focuses its attention on the effects due to the difference in this critical parameter.

The principal experimental tool being used here to examine behavior differences during fatigue is X-ray diffraction. In particular, the shapes of appropriate X-ray lines are examined through the Warren-Averbach [2] analyses so as to yield information on the root mean square microstrain and the particle size as a function of stress and number of fatigue cycles. The line shapes under study are recorded for samples of each alloy, fatigue at each of three maximum stress levels. The application of X-ray diffraction techniques to studies of damage in solid samples rather than in filings has not been widespread. Otte and his co-workers [3-7] have studied solid specimens deformed by wire drawing or by tension. Mikkola and Cohen [8] have applied Fourier analysis of diffraction peaks to solid specimens of ordered Cu_3Au deformed in tension. Hu *et al.* [9] applied the Fourier technique to both rolled and explosively shocked solid specimens of copper. In the area of electrodeposition a number of detailed X-ray studies have appeared [11, 12, 13] which utilize Fourier analysis of peak shapes. In the area of fatigue there are only two groups, other than the present one, currently performing X-ray studies. One is that of Evans [14, 15, 16] which has been performing Fourier analysis of X-ray line broadening in steels and the other is that of Taira [17] which has examined fatigue with film techniques including microbeam studies in steels, copper alloys and light alloys.

The other main measurement of this investigation is the fatigue striation spacing on the fracture face of samples representing the various stresses and compositions. Fatigue striations tell one the distance a fatigue crack propagates per cycle.

Experimental procedure

Binary alloys of 20·6 and 59·8 wt % Co in Ni (hereafter referred to as 20 and 60% Co) were rolled and annealed to give average grain diameters of 4×10^{-4} and $2{\cdot}5\times10^{-4}$ in respectively. Constant maximum stress plane bending fatigue specimens (Sonntag Corporation drawing No. 90881-S, spec. No. 1) were machined for testing in a Sonntag SF-2U fatigue machine. These were electropolished and cycled at maximum fiber stresses of 28,000, 45,000 and 60,000 psi. X-ray spectra were recorded with a G.E. XRD-5 at various intervals of fatigue life using Co Kα radiation for peaks through (222) and Mo Kα for (400). Rachinger's [18] graphical method was used to separate Kα_1 contributions from all peaks for Fourier analysis by the Warren-Averbach [2] method. A computer program due to DeAngelis [19] was used with a Univac 1108 computer to perform the Fourier deconvolutions of the observed spectra. Plots of normalized Fourier cosine coefficients were made against $ho^2=(h^2+k^2+l^2)$

for first and second order reflections in the ⟨111⟩ direction; (111) – (222) and in the ⟨100⟩ direction; (200) – (400). The initial slope of these curves gave the mean square micro strain over different averaging distances (L) below the surface and normal to the diffracting planes.

Plots of the $ho^2=0$ intercepts or particle size coefficients A_L^P of the above graphs versus L adjusted to pass through $A_L^P=1$ at $L=0$, yielded the particle size by extrapolating initial slopes to the L axis.

Inverse pole figures were determined as described by Sturken and Duke [20] for the two alloys prior to fatigue and are shown in Fig. 1.

Carbon replicas shadowed with Cr or Ge were taken of all fracture surfaces and examined in a Phillips E.M. 100 electron microscope.

Results and discussion

An earlier study [21] of fatigue in the current alloy system performed at 20,000 psi showed that the amount of X-ray line broadening at that stress was insufficient to allow deconvolution of fatigued peak profiles. Still later work [22] revealed that in samples fatigued directly to failure at any of the stress levels 28,000, 45,000 or 60,000 psi line broadening was insignificant. It was concluded at the time that in the latter case where the stress should be high enough to cause broadening, it may actually oscillate in magnitude during cycling, as in the work of Ogilvie and Moll [23] on pure Ni and not be well represented in the fractured condition. In the current work then fatigue was interrupted during cycling to avoid this possibility as well as to avoid having to perform X-ray work on a fractured and possibly bent sample. So far the 60,000 and the 45,000 psi stress levels have been re-examined and it is found that the optimum level for significant broadening is 45,000 psi. The remainder of this paper, therefore, will be devoted to considerations of fatigue at this stress.

Electron fractographs of samples fractured at 45,000 psi show that the average fatigue striation spacing is 1·6 microns for the 20% Co alloy and 0·38 microns for the 60% Co alloy. More of these figures later.

With regard to the X-ray line broadening, Fig. 2 shows that the particle size decreases from approximately 1200 Å (extrapolating the dotted curve) to 450 Å over 180,000 cycles. For discussion purposes let us call this a rate of decrease of 0·0042 Å/cycle. Fig. 2 shows that in the ⟨100⟩ direction the particle size decreases from about 800 to 690 Å in 180,000 cycles or a rate of decrease of 0·0006 Å/cycle. If we now go to Fig. 3 and first consider the ⟨111⟩ direction, the rate of decrease is approximately 0·05 Å/cycle and in the ⟨100⟩ direction there is probably no change at all. The following table summarizes this information.

It is apparent that almost independent of crystallographic direction and composition all particle sizes arrive close to 500 Å just prior to fracture.

It is also clear that for both alloys the rate of decrease of the particle size is not isotropic but always much faster in ⟨111⟩ than in ⟨100⟩; furthermore, in the 20% Co alloy, the rate of change of particle size in the ⟨111⟩ direction is an order of magnitude greater than in the 60% Co alloy. This fact is consistent with the greater mobility of extended dislocations in the 20% Co alloy (i.e. higher stacking fault energy).

Let us now express the striation spacing in terms of the average over-all particle size (500 Å) just before fracture. For the 20% Co alloy 1·6 microns is approximately 32 times 500 Å and for the 60% Co alloy 0·4 microns is approximately 8 times 500 Å, or for the high stacking fault energy alloy, the crack advances 32 cells versus 8 cells for the other. This says that in the high stacking fault energy alloy a crack advances 4 times as far per cycle as in the low stacking fault alloy. But how do the values of $\gamma_{S.F.}$ compare? It happens that $\gamma_{S.F.}$ is 4 times higher in the 20% Co alloy than in the 60% Co alloy [1]. This may be a fortuitous coincidence, however, if it proves to be reproducible and broadly applicable, then a very interesting and fundamental connection between substructure and external fracture face morphology will be established.

Figs. 5 and 6 show the r.m.s. microstrains for the 60% Co alloy in the ⟨111⟩ and ⟨100⟩ directions respectively during fatigue at 45,000 psi as a function of depth normal to these diffracting planes. No dramatic changes appear as a function of number of cycles. The strains along ⟨100⟩ are in general slightly higher than those along ⟨111⟩. The reason for this is not clear since a comparison of Figs. 2 and 3 shows that the particle size along ⟨111⟩ decreased to below that along ⟨100⟩ which might lead one to expect the microstrains along ⟨111⟩ to be higher than along ⟨100⟩. However, the difference here may be just experimental scatter. Agreement with expectation is better in Fig. 7 in that the ⟨111⟩ microstrains are all lower than the ⟨100⟩ microstrains as expected from the 40,000 cycle values on Fig. 4.

The exact reasons why the stacking fault energy is related to the distance traveled per cycle by a crack are yet unknown. We intend performing transmission electron microscopy on fatigued samples to attempt to elucidate this point as well as to confirm the above reported particle size results.

Conclusions

1. A one to one proportionality exists between $\gamma_{S.F.}$ and the distance traveled by a fatigue crack per cycle in Ni-Co alloys during cycling at 45,000 psi maximum fiber stress.

2. A limiting particle size of approximately 500 Å is reached just prior to fracture, independently of crystallographic direction or composition, during fatigue cycling at 45,000 psi.

3. The particle size decreases nearly an order of magnitude faster along ⟨111⟩ than along ⟨100⟩ in the 60% Co alloy.

4. The particle size along ⟨111⟩ in the 20% Co alloy decreases over an order of magnitude faster than does the particle size along ⟨111⟩ in the 60% Co alloy.

Acknowledgements

This study has been supported by the U.S. National Science Foundation and the alloy materials were provided by the International Nickel Company. Much past assistance from Dr J. B. Cohen and Dr R. J. DeAngelis of Northwestern University and the University of Kentucky, respectively, was invaluable.

References

1. DILLAMORE, I. L., private communication, 1965.
2. WARREN, B. E., *Progress in Metal Physics*, vol. 8, 1959, p. 147.
3. OTTE, H. M., *J. Appl. Phys.*, vol. 32, 1961, p. 1536.
4. OTTE, H. M., *J. Appl. Phys.*, vol. 33, 1962, p. 2892.
5. OTTE, H. M. and WELCH, D. O., *Phil. Mag.*, vol. 8, 1963, p. 345.
6. OTTE, H. M., Advances in X-ray analysis, vol. 6, 1963, Editors W. M. Mueller and M. Fay, Plenum Press, New York.
7. OTTE, H. M. and WELCH, D. O., *Phil. Mag.*, vol. 9, 1964, p. 299.
8. MIKKOLA, D. and COHEN, J. B., *Acta Met.*, vol. 14, 1966, p. 105.
9. HU, H., CLINE, R. S. and GOODMAN, S. R., *J. Appl. Phys.*, vol. 7, 1961, p. 1392.
10. DEANGELIS, R., Ph.D. Thesis, 1964, Northwestern University.
11. HINTON, R. W., SCHWARTZ, L. H. and COEHN, J. B., *J. Electrochem. Soc.*, vol. 110, 1963, p. 103.
12. HOFFER, E. and HINTERMANN, H. E., *J. Electrochem. Soc.*, vol. 112, 1965, p. 167.
13. HOFFER, E. and HINTERMANN, H. E., *Trans. Faraday Soc.*, vol. 60, 1964, p. 1457.
14. EVANS, W. P. and MILLAN, J. F., SAE Congress, Detroit, Michigan, 1964, p. 793B.
15. EVANS, W. P. and BUENNEKE, *Trans. A.I.M.E.*, vol. 227, 1963, p. 447.
16. EVANS, W. P., RICKLEFS, R. E. and MILLAN, J. F., *Local atomic arrangements studied by X-ray diffraction*, 1966. Gordon and Breach, New York.
17. TAIRA, S., *International Conf. on Fracture*, 1965, Sendai, Japan.
18. RACHINGER, W. A., *J. Sci. Inst.*, vol. 25, 1948, p. 254.
19. DEANGELIS, R. J., *Local atomic arrangements studied by X-ray diffraction*, p. 271, 1966, Gordon and Breach, New York.
20. STURKEN, E. F., and DUKE, W. G., U.S.A.E.C. Contract AT(07-2)-1, Savannah River Laboratory, 1961.
21. VANDERSANDE, J. B. and BYRNE, J. G., *Transactions Quart. A.S.M.*, vol. 60, 1967, p. 543.
22. SOUTHERN, B. and BYRNE, J. G., unpublished results.
23. OGILVIE, R. E. and MOLL, S., INCO, Inc., seminar, March 22, 1960, Duquesne Club, Pittsburgh, Pennsylvania.

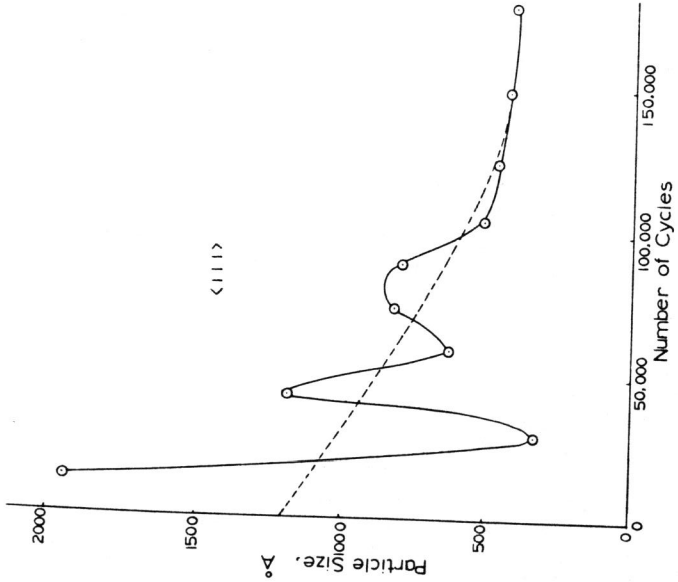

Fig. 2. Particle size (Å) for the 60% Co alloy along ⟨111⟩ for fatigue at 45,000 psi.

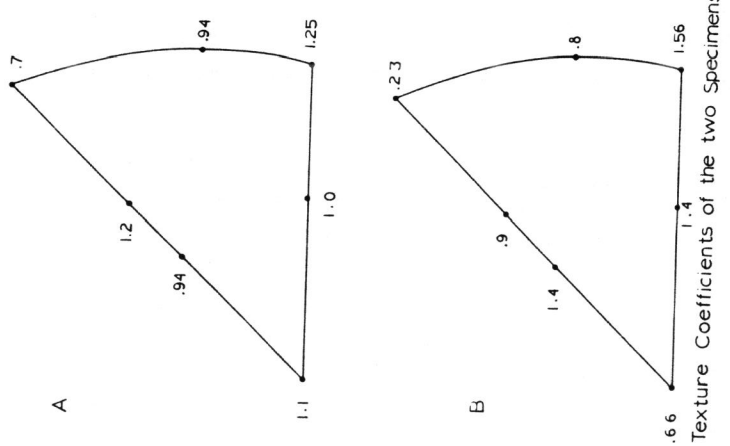

Fig. 1. Inverse pole figures for the 20 and 60% Co materials prior to fatigue. (A) 20% Co; (B) 60% Co.

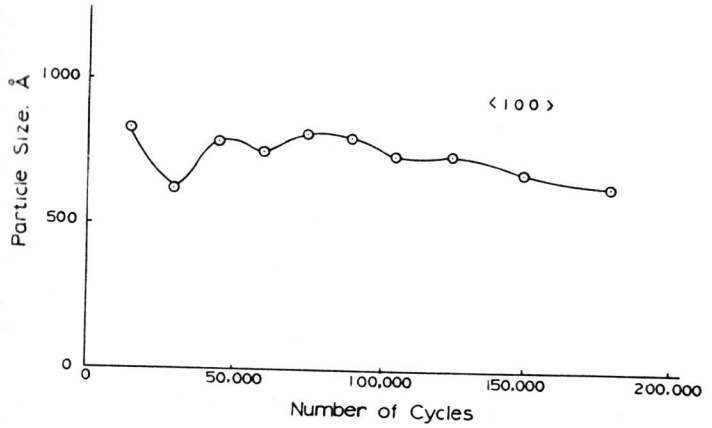

Fig. 3. Particle size (Å) for the 60% Co alloy along ⟨100⟩ for fatigue at 45,000 psi.

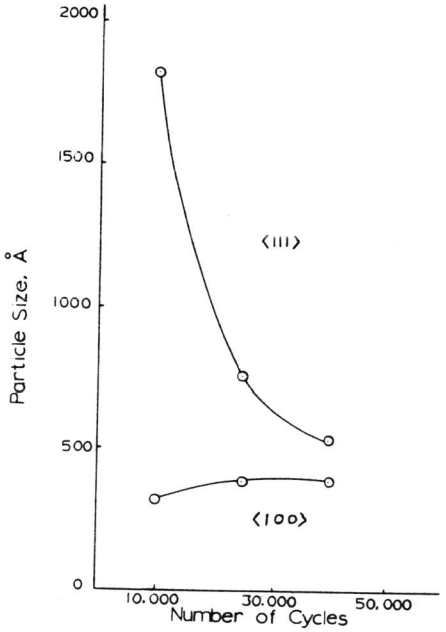

Fig. 4. Particle size (Å) for the 20% Co alloy in the ⟨111⟩ and ⟨100⟩ directions for fatigue at 45,000 psi.

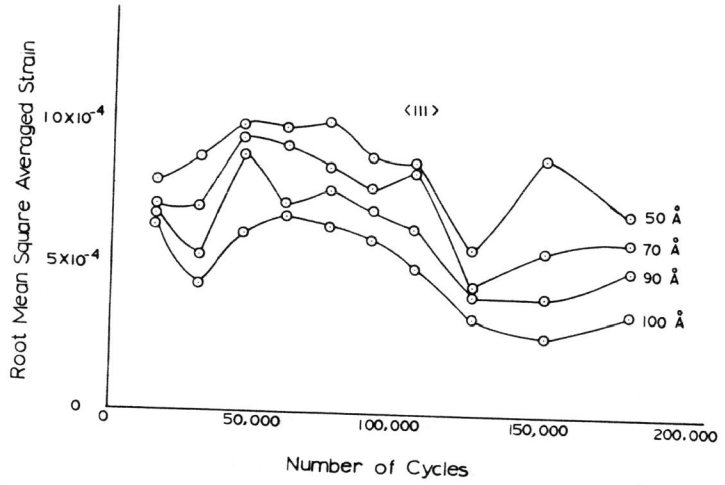

Fig. 5. Root mean square average microstrain along ⟨111⟩ at various depths perpendicular to the diffracting planes for 60% Co alloy during fatigue at 45,000 psi.

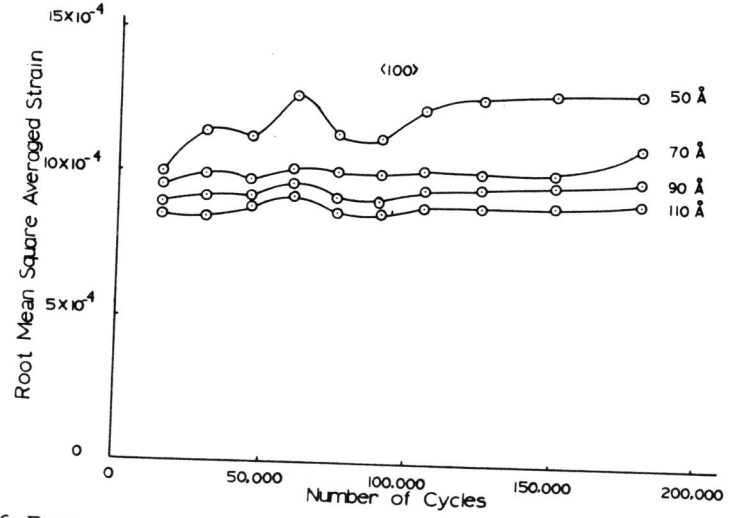

Fig. 6. Root mean square average microstrain along ⟨100⟩ at various depths perpendicular to the diffracting planes for the 60% Co alloy during fatigue at 45,000 psi.

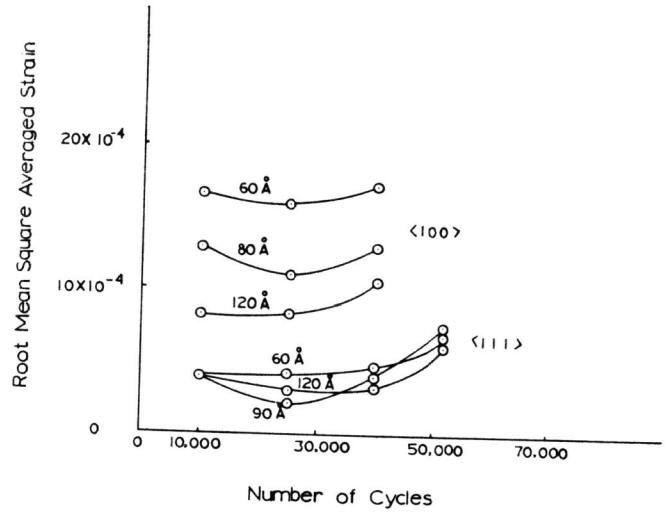

Fig. 7. Root mean square average strains along ⟨100⟩ and along ⟨111⟩ for 20% Co alloy at various depths perpendicular to these diffracting planes during fatigue at 45,000 psi.

Table 1

Alloy	*Direction*	*Rate of decrease of particle size (Å/cycle)*	*Particle size just prior to fracture (Å)*
60% Co	⟨111⟩	0·0042	430
	⟨100⟩	0·0006	625
20% Co	⟨111⟩	0·0500	520
	⟨100⟩	zero	400
		Average	494 Å